Carbon Letters (2023) 33:1629–1638
https://doi.org/10.1007/s42823-023-00529-9

Online ISSN 2233-4998
Print ISSN 1976-4251

ORIGINAL ARTICLE

N, S co-doped fluorescent carbon dots synthesized by microwave irradiation: a sensitive probe for Pb (II) ions detection in food samples

Elias Aboobakri[1] · Tahereh Heidari[1] · Moslem Jahani[2]

Received: 30 January 2023 / Revised: 19 April 2023 / Accepted: 10 May 2023 / Published online: 31 May 2023

Abstract

Sulfur and nitrogen co-doped carbon dots (NSCDs) were quickly synthesized by the microwave-assisted method from tri-ammonium citrate and thiourea. NSCDs showed a quantum yield of 11.5% with excitation and emission bands at 355 and 432 nm, respectively. Also, a fluorescence quenching was observed in the presence of Pb(II) ions, and the as-synthesized CDs were used as a sensitive probe for detecting Pb(II) in water and food samples. The results showed the optimal conditions for Pb(II) determination were CDs concentration of 0.02 mg mL^{-1} at pH 6.0–7.0 and an incubation time of 20 min. The relative fluorescence intensity of NSCDs was proportional to Pb(II) concentrations in the range of 0.029–2.40 and 2.40–14.4 μmol L^{-1} with a correlation coefficient (R^2) of 0.998 and 0.955, respectively, and a detection limit of 9.2×10^{-3} μmol L^{-1}. Responses were highly repeatable, with a standard deviation below 3.5%. The suggested method demonstrates the potential of a green, fast, and low-cost approach for Pb(II) determination in water, tea, and rice samples with satisfying results.

Keywords Carbon-dots · Pb(II) · Microwave-assisted synthesis · Heavy metals · Fluorescent quenching · Food samples

Abbreviations

AAS	Atomic absorption spectrometry
CDs	Carbon dots
DLS	Dynamic light scattering
EtOH	Ethanol
FL	Fluorescence
ICP-MS	Inductively coupled plasma-mass spectrometry
ICP-OES	Inductively coupled plasma-optical emission spectrometry
MeOH	Methanol
QDs	Quantum dots
QY	Quantum yield
SEM	Scanning electron microscope
TAC	Tri-ammonium citrate
TEM	Transmission electron microscope

✉ Tahereh Heidari
taherehheidari@um.ac.ir

Moslem Jahani
m.jahani@RIFST.ac.ir

[1] Department of Chemistry, Faculty of Sciences, Ferdowsi University of Mashhad, P.O. Box: 9177948974, Mashhad, Iran

[2] Department of Food Chemistry, Research Institute of Food Science and Technology (RIFST), Mashhad, Iran

1 Introduction

Different industrial activities lead to the widespread release of contaminated effluents into the environment, which poses a significant threat to human health [1]. Pollution of food and water resources with heavy metals has become a significant threat in today's world that has been frequently reported. Therefore, monitoring toxic heavy metals in different samples has become a global issue in health organizations [2].

Owing to their non-biodegradable nature, heavy metals can readily be accumulated in biological systems. Lead (Pb) is one of the most common toxic heavy metals, with widespread industrial applications [3]. According to the EPA specification (US Environmental Protection Agency), lead is a probable human carcinogen that can damage human organs and systems. Concentrations higher than 5.0 μmol L^{-1} in the blood can cause adverse health-related problems, particularly for children. Exposure to high concentrations of Pb(II) can severely damage the brain and kidneys and even cause death to human beings [4]. So, tracking heavy metal concentrations like Pb(II) is highly required in soil, water, and food samples.

Atomic absorption spectrometry (AAS), inductively coupled plasma in combination with optical emission spectrometry (ICP-OES) or mass spectrometry (ICP-MS), and electrochemical techniques are commonly used methods

for the determination of heavy metals [5]. They are entirely practical methods but suffer disadvantages such as expensive and sophisticated instruments, the need for expert operators, long measuring periods, and limited applications for on-site determinations. So, developing inexpensive, accurate, rapid, and portable detection methods is highly demanded. Recently, fluorescence-based sensors have received remarkable attention as alternative detection strategies [6] with the advantages of cost-effectiveness, sensitivity and specificity, real-time monitoring, and fast responses [7]. Various sensors have been reported for Pb(II) detection in water and food samples. Modified multi-walled carbon nanotubes were used to develop a new selective electrochemical sensor for Pb(II) detection in water and standard alloy samples. The new sensor showed a linear range of 0.9–114.6 μg L^{-1} [5]. A colorimetric chemosensor based on a paper test-strip platform and smartphone detection was also proposed to determine lead ions. The chemosensor strip was functionalized with gold nanoparticles to enhance the colorimetric response. Under the optimal conditions, the color intensity of the chemosensor strip increased linearly with the Pb(II) concentrations in the range of 0.1–1.0 mg L^{-1}. The paper test strip was successfully applied for Pb(II) analysis in meat samples [8]. Also, an electrochemical sensing platform was proposed based on the binary assembly of silica nanochannels and polydimethylsiloxane and evaluated to detect Pb(II) and Cd(II). The method showed linear ranges of 4–1500 μg L^{-1} for Pb(II) and 30–900 μg L^{-1} for Cd(II). Quantitative detection of Pb(II) and Cd(II) in real juice and beverage samples was also performed without tedious pretreatments [9].

A sensitive fluorescent probe was developed based on functionalized molybdenum disulfide quantum dots (QDs) and used for monitoring lead ions in an aqueous medium [10]. QDs are highly fluorescent semiconductors with characteristics of size-tunable emission and high fluorescence quantum yield. However, high toxicity limits their use in most cases, like biological applications. Over the past few years, carbon dots (CDs) were introduced as a new class of fluorescent nanoparticles. Fluorescent carbon dots usually have a spherical structure smaller than 10 nm and exhibit intense and stable fluorescence [11, 12]. Other promising properties of CDs, like aqueous solubility, low toxicity, and biocompatibility, make them suitable candidates to replace QDs [13]. CDs can be prepared from different cheap and available raw materials. Also, scientific reports concerning metal ions and biological molecules detection based on CDs are increasing, and investigating synthesis methods, functionalization, and their application as fluorescent sensors are highly required.

Fluorescent CDs can be synthesized through different strategies such as arc discharge, laser ablation, electrochemical oxidation, acidic oxidation, combustion, hydrothermal treatment, ultrasonic treatment, and microwave-assisted methods [11, 14]. The hydrothermal synthesis route is an efficient but time-consuming procedure. Recently, microwave-assisted pyrolysis has been introduced as a fast synthesis method with the advantages of low energy consumption, strong sustainability, short reaction time, and high yield [15]. Also, the quantum yield improvement was taken into consideration by hetero-atom doping in CDs.

The present study explains the synthesis of N, S co-doped carbon dots (NSCD-1, NSCD-5, and NSCD-10) with different sulfur content (1, 5, and 10%wt) by a fast microwave-assisted method. Tri-ammonium citrate and thiourea (CH_4N_2S) were used as sources of doping elements (core doping) to enhance fluorescence properties. The preparation method has the advantages of a simple apparatus, mild reaction conditions, and low cost. The newly synthesized CDs were used to establish a ratiometric fluorescence probe for Pb(II) ions detection. A reduction of fluorescence intensity was observed in the presence of Pb(II), which proves the possibility of monitoring the amount of Pb(II) based on fluorescence quenching. The sensing strategy was validated in water samples and used as a sensitive sensor for Pb(II) determination in food samples.

2 Materials and methods

2.1 Instrumentation

Fluorescence (FL) determinations were performed with Cary Eclipse Fluorescence Spectrophotometer (Agilent, USA) equipped with a Xenon lamp and 10.0 mm quartz cell. Ultraviolet–visible spectra (200–800 nm) were recorded on a DR 500 UV–Vis spectrophotometer (Hach, USA). The surface functional groups and size distribution profiles of the as-synthesized CDs were investigated through Fourier transform infrared (FT-IR) and dynamic light scattering (DLS) analysis. The infrared spectroscopic measurements (4000–400 cm^{-1}) were performed on a thermo-Nicolet (AVATAR 350) FT-IR spectrometer. DLS analysis was performed using the Horiba SZ-100 particle size analyzer (Horiba Scientific, Japan). The surface morphology of the product was analyzed by a scanning electron microscope (SEM model Stereoscan 360, Cambridge Scientific Instrument Company, Britain) equipped with energy-dispersive X-ray (EDX) chemical analysis. The physical morphology and dispersity of the synthesized CDs were observed using a transmission electron microscope (TEM, LEO, 912AB).

2.2 Chemicals and reagents

Tri-ammonium citrate (TAC), dipotassium hydrogen phosphate (K_2HPO_4), thiourea, nitric acid, sulphuric acid, sodium hydroxide, and Pb(II) nitrate were purchased from Sigma

(Missouri, USA). Ethanol (EtOH), methanol (MeOH), acetone, quinine sulfate, and other chemicals were obtained from Merck (Darmstadt, Germany). All chemicals were analytical grade and used directly without any purification. The aqueous solutions were prepared in ultrapure water (resistivity of 18.2 MΩ cm^{-1}) obtained from an Aqua Max ultrapure water system (Young Lin, Korea).

2.3 Preparation of carbon dots

The highly fluorescent CDs were synthesized according to earlier work using tri-ammonium citrate and thiourea as carbon and sulfur sources, respectively [16]. Briefly, tri-ammonium citrate (1.00 g) and dipotassium hydrogen phosphate (0.20 g) were dissolved in 2.5 mL ultrapure water. Afterwards, thiourea was added and the final solution was sonicated for 5 min. The solution was irradiated for 2.5 min in a domestic microwave oven (Panasonic, model NN-GD692) at 400 W, and a brownish-yellow solid powder was obtained. After natural cooling to room temperature, the product was crushed and washed with anhydrous ethanol (20 mL × 3 times). The obtained CDs were dissolved in water and dialyzed against ultrapure water for 24 h. Finally, the purified solid sample was obtained by evaporating the solvent at 40 °C. The CDs, with excellent water solubility, were stored at 4 °C for advanced analysis. The synthesis route was repeated with 0.01, 0.05, or 0.1 g of thiourea to yield a final concentration of 1, 5, or 10%wt of the sulfur source.

The fluorescence intensity of the prepared carbon dots was evaluated in the presence of different metal ions. Here, 0.1 mL CDs solution (0.5 mg mL^{-1}) was mixed with 1.0 mL of metal ion standard solution (10 mg L^{-1}) and diluted to 5.0 mL with deionized water (with different pH). The samples were sonicated for 20 min, and fluorescence emission spectra were recorded under excitation at 355 nm.

2.4 Quantum yield calculation

The quantum yield (QY) of the synthesized NSCDs was calculated using quinine sulfate as the reference material [17]. Quinine sulfate (literature QY = 0.54) was dissolved in 0.1 mol L^{-1} H_2SO_4 (refractive index (η) of 1.33), while the CDs were dissolved in water ($\eta = 1.33$). The fluorescence spectra of quinine sulfate and carbon dots solutions and their absorbance were recorded at 355 nm. The quantum yield was calculated according to Eq. (1).

$$QY_{CDs} = QY_R\left(\frac{m_{CDs}}{m_R}\right)\left(\frac{\eta_{CDs}^2}{\eta_R^2}\right) \quad (1)$$

where QY is the quantum yield, m is the slope of luminescent intensity vs. absorbance curve, and η is the refractive index of the solvent. The subscripts of CDs and R are used for carbon dots and reference, respectively.

2.5 Fluorescence measurement of Pb(II) ions

Into a 5.0 mL volumetric flask, 0.1 mL of CDs aqueous solution (1.0 mg mL^{-1}) was transferred with an appropriate quantity of Pb(II) stock solution and diluted with deionized water (adjusted to pH 6.0–7.0). The final concentration of Pb(II) was in the range of 0.029–14.4 µmol L^{-1}. The resulting mixtures were sonicated for 20 min at room temperature (23.0–25.0 °C). The fluorescence emission spectra were recorded using an excitation wavelength of 355 nm and an emission range of 300–600 nm (maximum fluorescence emission at 432 nm). The quenching of the fluorescence signal was considered with the Stern–Volmer equation (Eq. 2):

$$\frac{FL_0}{FL} = 1 + K_{SV}[C] \quad (2)$$

In this equation, FL and FL_0 are fluorescence intensities of NSCDs in the presence and absence of Pb(II), K_{SV} is the Stern–Volmer constant, and [C] is the concentration of the analyte [13].

2.6 Effects of coexisting ions

A series of ions (Na^+, Ag^+, Ca^{2+}, Mg^{2+}, Cd^{2+}, Co^{2+}, Ni^{2+}, Mn^{2+}, Zn^{2+}, Cu^{2+}, Hg^{2+}, Fe^{3+}, As^{3+}, Al^{3+}) were examined for the selectivity evaluations. In a 5.0 mL volumetric flask, 0.1 mL of CDs stock solution (1 mg mL^{-1}), 1.0 mL Pb(II) standard solution (2.5 µmol L^{-1}), and a quantity of a coexisting ion were mixed and diluted with deionized water (adjusted to pH 6.0–7.0). The final concentration of each coexisting ion was changed in the range of 0.50–50 µmol L^{-1}. The resulting mixtures were sonicated for 20 min, and FL spectra were recorded at the excitation wavelength of 355 nm. The tolerance limit was defined as the concentration ratio of the coexisting ion to Pb(II) that changes the FL intensity of NSCDs lower than 10%.

2.7 Treatment of real samples

The mineral and potable water samples were filtered using a 0.45 µm membrane filter and then spiked with Pb(II) standard solution at different concentrations [18]. Then, 0.1 mL of CDs stock solution (1 mg mL^{-1}) and 1.0 mL of real sample were transferred to a volumetric flask (5.0 mL) and diluted with deionized water (adjusted to pH 6.0–7.0). Finally, the mixtures were sonicated and measurement was carried out as described in Sect. 2.5. The commercially available rice and tea samples were purchased from the local markets in Mashhad in March 2019. Food samples were mineralized

following usual laboratory procedures [19]. We proceeded to spike food samples with Pb(II) at the obtained linearity range and the applicability of the analytical assay was studied by the standard addition method.

3 Results and discussion

3.1 Synthesis and characterization of CDs

The present study explains the synthesis of water-soluble and fluorescent CDs through a simple microwave-assisted procedure. Tri-ammonium citrate and thiourea were used as carbon and sulfur sources, respectively. The fluorescence intensity of CDs was increased with an increase in the amount of thiourea (Supporting information Fig. S1). However, NSCD-5 showed significant quenching in the presence of Pb(II) ions and better selectivity to Pb(II) compared to other investigated ions (Fig. 1a–c). Pb(II) may simultaneously combine with several nitrogen and sulfur atoms of NSCDs. This complexation process may lead to the formation of aggregates and a change in the electronic structure of carbon dots [20]. The fluorescence quenching is caused by the formation of a non-luminescent connection between NSCDs and Pb(II) ions as electron donors and acceptors, respectively [21–23].

Figure 1a–c shows the effect of different metal ions on the emission intensity of the synthesized CDs at different initial pH values. The metal ions have the same concentrations of 2.0 mg L^{-1}. Only Pb(II) caused a significant decrease in the fluorescence intensity of NSCD-5, while other ions maintained up to more than 80% of the initial fluorescence intensity. Also, NSCD-10 showed the lowest quenching and similar results for different metal ions (low selectivity). According to the results, fewer interferences are expected with NSCD-5 for Pb(II) detection in the presence of other ions like Fe and Hg. It reflects that NSCD-5 can be used to develop a Pb(II) ion sensor. The results also showed a significant influence of pH on the fluorescence quenching effect of metal ions.

The UV–Vis spectra of CDs (Fig. 2a) showed a characteristic peak at 226 nm, assigned to the π–π* electronic transitions of C=C double bonds forming the carbon core. An absorbance peak around 325 nm corresponds to the n–π*

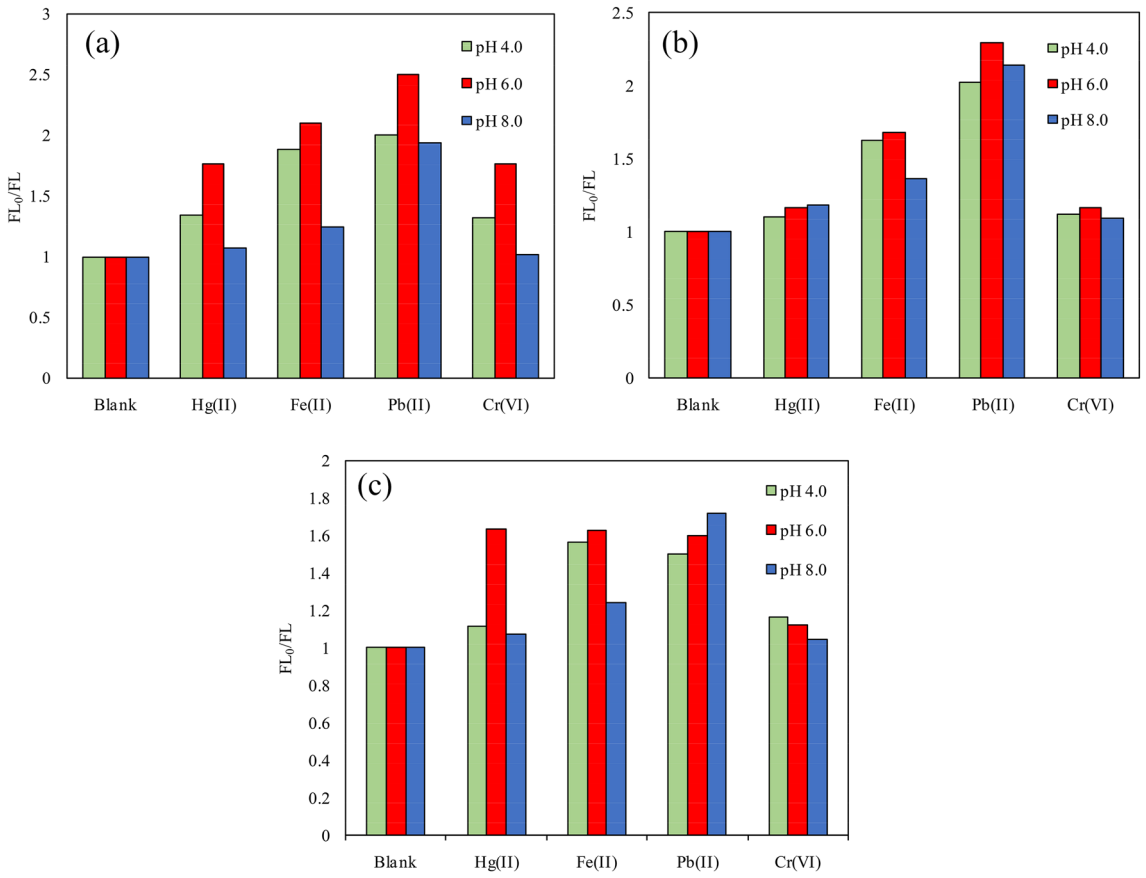

Fig. 1 The effect of different metal ions and pH on the emission intensity of CDs synthesized at the presence of 1%wt (**a**), 5%wt (**b**), and 10%wt of thiourea (**c**). [Conditions: CDs, 20 μg mL^{-1}; metal ion, 2 mg L^{-1}; Excitation and emission at 355 and 432 nm, respectively]

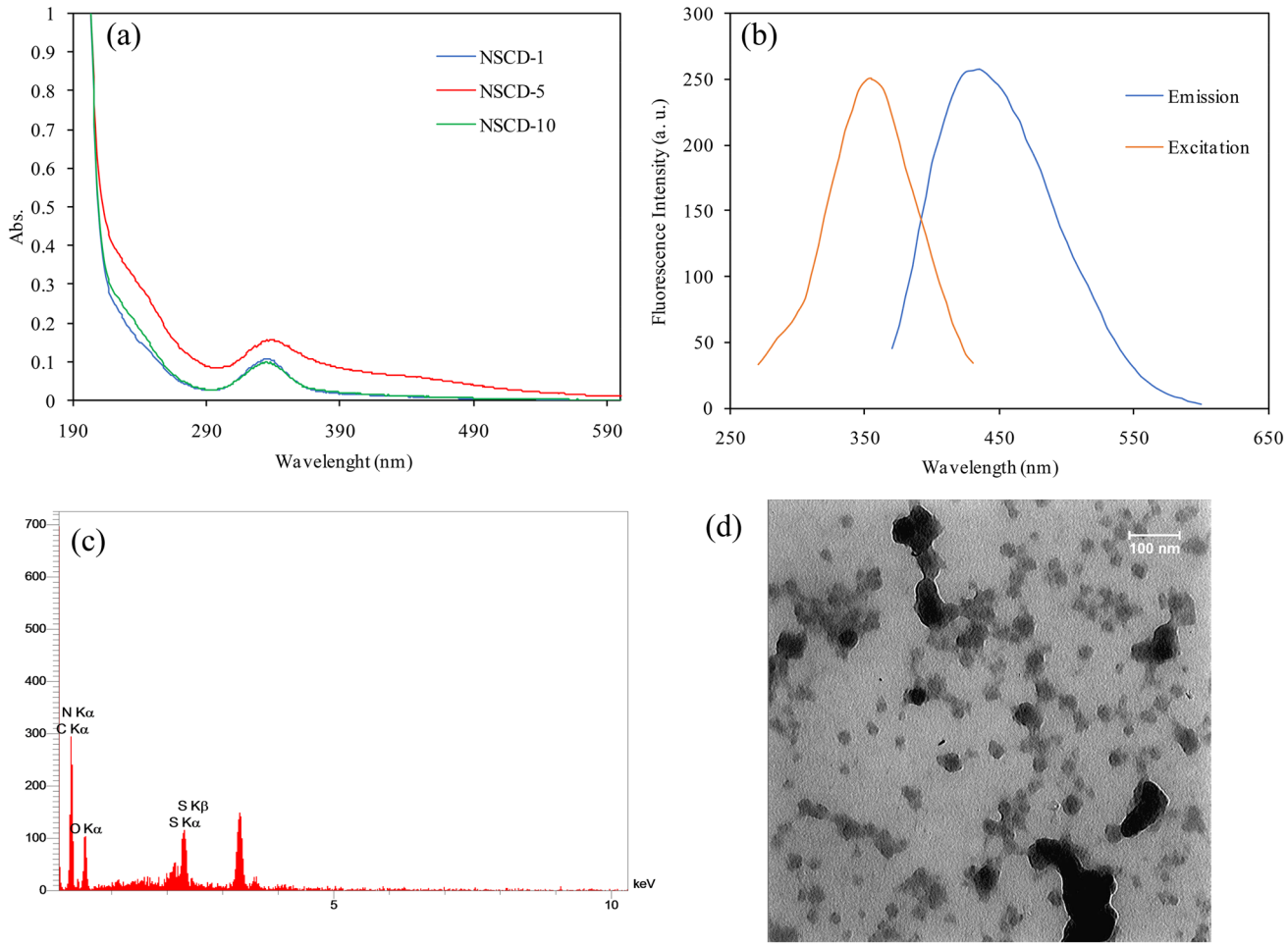

Fig. 2 UV–Vis absorption spectra of CDs (**a**), excitation-emission spectrum (**b**), EDX analysis result (**c**), and TEM image of NSCD-5 (**d**)

electronic transitions of C=N and C=O bands originating from the surface of CDs. However, it should be noted that variation in surface functional groups results to change in UV–Vis absorption spectra [24, 25]. As presented in Fig. 2b, the NSCDs-5 exhibited a strong emission at 432 nm when excited at 355 nm, corresponding to the blue fluorescence [26].

The emission spectra of NSCDs were also investigated at different excitation wavelengths ranging from 330 to 360 nm with an increment of 5 nm. The maximum fluorescent intensity was first increased and followed by a decrease accompanied by a gradual red-shift (Supporting information Fig. S2). Such excitation-dependent emission property has been reported as a characteristic of CDs attributed to the distribution of different emissive sites on each nanoparticle [27]. So, an excitation wavelength of 355 nm was fixed in the following experiments for the most intensive fluorescence emission. The QY for the prepared NSCD-5 is found to be 11.5%.

The elemental composition of the NSCD-5 sample was also characterized by the energy-dispersive X-ray (EDX) analysis (Fig. 2c). The results indicated the successful doping of nitrogen and sulphur into the CDs, with an elemental composition of 59.57, 13.99, 24.30, and 2.13%wt of C, N, O, and S. Also, the corresponding DLS size distribution analysis (Supporting information Fig. S3) showed a size distribution of 13 to 90 nm with a mean size of 27 nm (Dv50). The TEM images showed that NSCD-5 are not in regular shape with monodispersity, and the estimated average size of CDs was about 20–70 nm (Fig. 2d).

The prepared carbon dots are readily water-soluble due to the presence of hydroxyl and carboxyl groups, confirmed by FT-IR analysis (Supporting information Fig. S4). The broadband in the 3060–3450 cm^{-1} region is assigned to the stretching vibrations of the O–H and N–H groups. The band at 2937 cm^{-1} could be identified as the C–H stretching vibrations [28]. The peaks around 1590 and 1715 cm^{-1} were attributed to the bending vibration of N–H and the stretching vibrations of C=O, respectively [29]. The peak at 1400 cm^{-1} could be identified as C–N, N–H, and –COO groups [30]. The results confirm the presence of carboxylic acid and other

oxygen-containing functional groups. The absorption bands at 2060 cm^{-1} are assigned to the vibration of N=C=S bonds, indicating that S and N atoms have been doped into CDs.

The FT-IR spectra of the Pb(II)-loaded CDs showed differences in the intensity and position of the main characteristic bands of CDs, mainly at 2760, 2060, and 1590 cm^{-1} (Fig. 3). Also, the IR peak centered at 1400 cm^{-1} showed a shift to 1370 cm^{-1}. All these confirm the interaction of NSCD-5 and Pb(II) ions.

3.2 Fluorogenic detection of Pb(II)

The results showed effective quenching of the fluorescence intensity of NSCDs in the presence of Pb(II) ions. It may be attributed to the chelating of Pb(II) by the surface functional groups of CDs and non-radiative recombinations through the electron transfer process [31, 32]. So, the as-synthesized CDs were evaluated as a turn-off chemosensor for Pb(II) ions. Then, the sensor responses were examined under different experimental settings of CDs concentration and pH to obtain the optimized conditions for Pb(II) determination.

Lower CDs concentrations can cause higher sensitivity, but a broader detection range can achieve at higher concentrations. The concentration of CDs was examined between 0.01 and 0.08 mg mL^{-1}. As presented in Fig. 4a, the CDs concentration has a significant effect on the Pb(II) detection. It is readily apparent that the value of FL_0/FL was initially increased with the increase of CDs amount followed by a reduction beyond 0.02 mg mL^{-1} of CDs. The loss of fluorescence intensity at high concentrations results from self-quenching. The fluorescence intensity of CDs is proportional to the concentration. However, similar to other fluorescent substances, CDs exhibit clear self-quenching effects. As the concentration increases, the fluorescence intensity decreases [33]. The synthesized CDs showed the potential to apply for Pb(II) ions detection based on the quenching effect. Accordingly, the initial intensity of CDs was optimized to the highest instrumentation scale, and the CDs concentration before self-quenching (0.02 mg mL^{-1}) was used for further studies.

Figure 4b exhibited the pH effect (in the range of 2.0–9.0) on the FL intensity of CDs. FL_0/FL was increased gradually and reached a maximum at pH 6.0–8.0. Reduction in the FL_0/FL at pH values lower than 6.0 may result from competition between Pb(II) and H_3O^+ ions for the surface active sites of CDs. Also, the interaction of hydronium ions and hydroxyl groups can reduce the fluorescence intensity of CDs. Hydrolysis and precipitation of Pb(II) can occur in basic solutions. Therefore, pH 6.0–7.0 was used as the optimal value.

3.3 Analytical features

The fluorescence intensity of the sensor was evaluated during the addition of different amounts of Pb(II) ions into the CDs solution under optimal conditions. As illustrated in Fig. 4c, a continuous decrease of FL intensity (or increase in FL_0/FL ratio) occurs in the range of 0.028–14.4 µmol L^{-1} of Pb(II). A closer look showed two linear regions between 0.028 and 2.40 µmol L^{-1} and 2.40–14.4 µmol L^{-1} with a correlation coefficient of 0.998 and 0.955, respectively (Fig. 4c). Based on the 3 s m^{-1} rule (s is the standard deviation of the blank signals ($n = 25$) and "m" is the slope of the calibration curve) the limit of detection (LOD) of 9.2 and 574 nmol L^{-1} was calculated for two separate linear regions [34, 35].

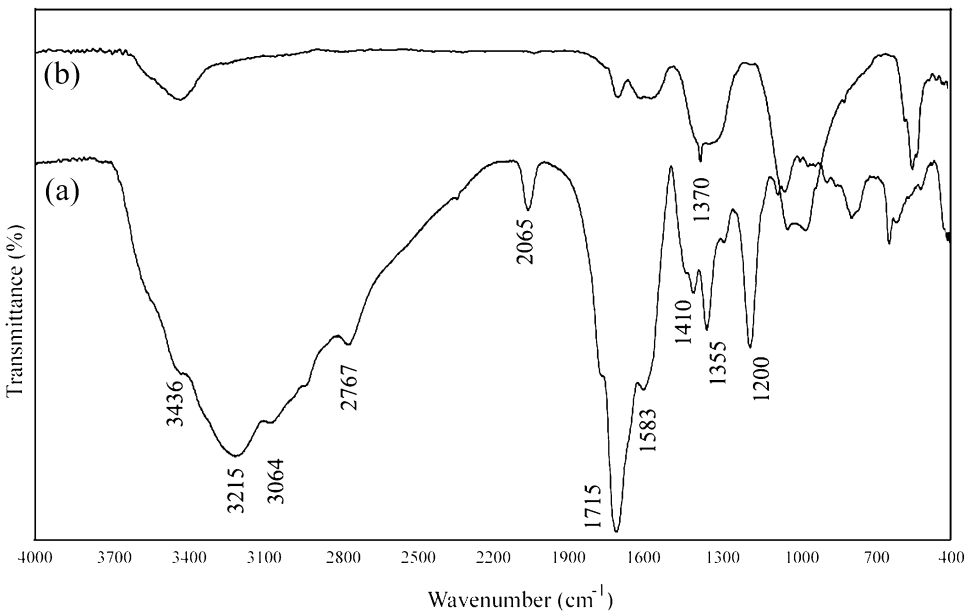

Fig. 3 FT-IR spectra of NSCD-5 (**a**) and Pb(II)-loaded NSCD-5 (**b**)

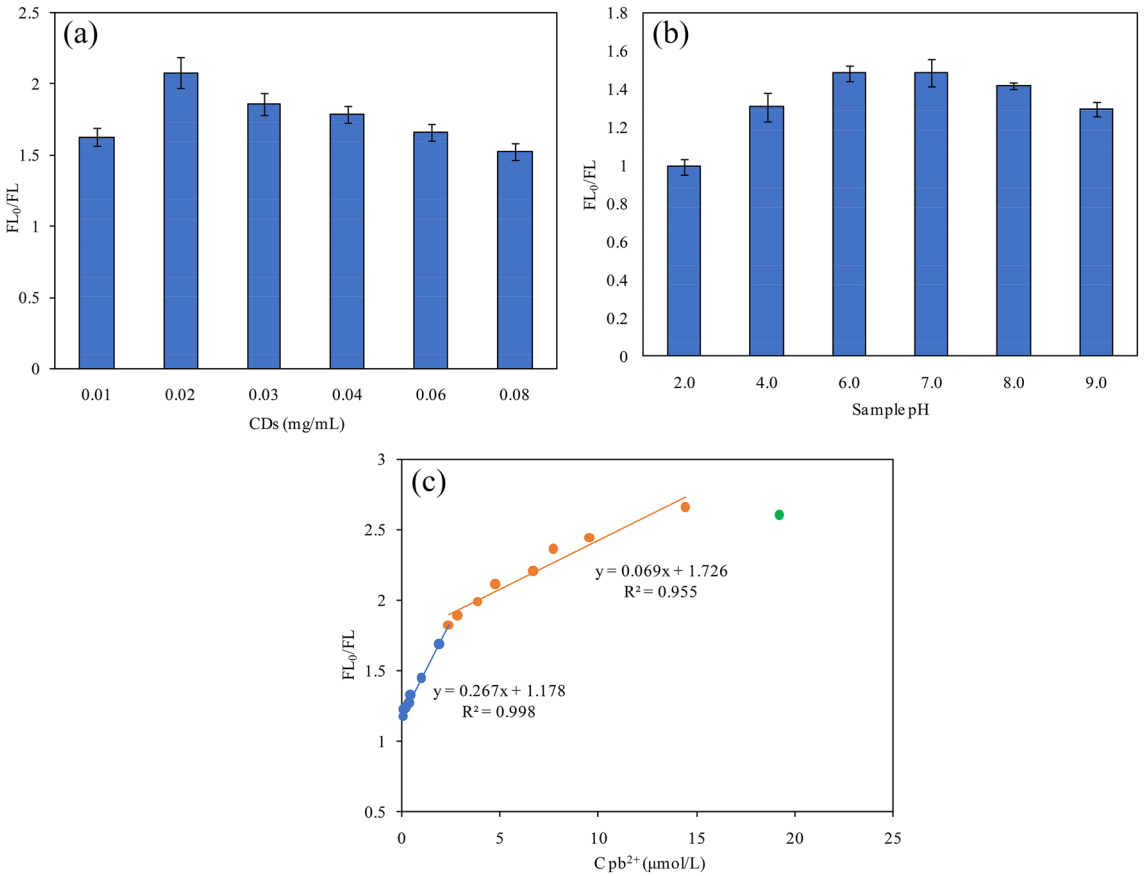

Fig. 4 The plot of the quenched fluorescence signal (FL_0/FL) **a** versus CDs concentration in the presence of Pb(II) ions (9.6 μmol L^{-1}), **b** versus pH in the presence of Pb(II) ions (2.9 μmol L^{-1}), and **c** the fluorescence response of NSCD-5 upon the addition of different concentrations of Pb(II)

In general, fluorescence quenching can result from dynamic or static quenching effects; both conform to the conventional Stern–Volmer equation [36]. As shown in Fig. 4c, the Stern–Volmer diagram was not a straight line but a curve, suggesting a combination of dynamic and static quenching for the detection mechanism of Pb(II) by NSCDs. The linear regression equation for Pb(II) was $FL_0/FL = 0.267\ [Pb(II)] + 1.178$ in the range of 0.028–2.4 μmol L^{-1} (Fig. 4c). The calculated Stern–Volmer dynamic quenching constant, *K*sv, is 2.67×10^5 L mol^{-1}.

A comparison between the present study and some previous documents shows that the introduced sensor is comparable to or even better in the linear range and LOD for Pb(II), with a much simpler and easier operation (Table 1). A fast and single-step method was also used to synthesize CDs under microwave irradiation. Therefore, the new chemosensor can be an excellent alternative method for monitoring Pb(II) ions.

Table 1 Comparison of different CDs-based sensors for the detection of Pb(II)

Chemosensor	Linear range (μmol L^{-1})	LOD (nmol L^{-1})	Refs.
Copper nanoclusters @ NCDs	0.048–12.0	15.00	[37]
NCDs	0.0167–1	4.60	[38]
CDs	0.5–11.0	8.47	[39]
BCDs[a]	0.025–250	2.00	[4]
CDs	Not given	5050	[13]
NCDs	0.1–6.0	15.00	[40]
CDs	0.033–1.67	12.70	[41]
NSCDs	0.028–2.40	9.20	This work
	2.4–14.4	574	

[a]Boron-doped carbon dots

3.4 Interference study

High selectivity, in addition to sensitivity, is another important advantage of a sensor. So, the sensor's responses

were evaluated for 0.50 µmol L^{-1} of Pb(II) and in the presence of some interfering ions (Supporting information Fig. S5). Metal ions of Na^{+}, Ca^{2+}, Mg^{2+} up to 100 times and Cd^{2+}, Cr^{6+}, Fe^{3+}, Hg^{2+}, As^{3+}, Co^{2+}, Ni^{2+}, Mn^{2+}, Zn^{2+}, Al^{3+} until to 20 times of Pb(II) ions concentration only caused minor fluorescence changes (lower than 10%). Significant interferences were observed for Ag^{+} and Cu^{2+} at concentrations ten times more than the concentration of Pb(II) ions. It can be explained by more affinity of surface functional groups to coordinate Pb(II) and strong binding with doped elements such as S and N [42].

3.5 Analysis of food samples

Considering the sensitivity and selectivity of the new sensor to Pb(II), the feasibility and reliability of the method were evaluated in water, tea, and rice samples. As presented in Table 2, no Pb(II) was found in the samples, and recoveries were between 96.5 and 107.0%. Also, a replicate analysis of a potable water sample spiked with Pb (0.50–2.4 µmol L^{-1}) showed RSD values of 2.21–3.52% ($n=3$). The results indicated that the developed method could be used as an alternative method to determine Pb(II) ions in real samples.

Table 2 Determination of Pb(II) in water and food samples

Sample	Spiked level (µmol L^{-1})	Found (µmol L^{-1})	Recoveries (%)
Bottled water (Aqua)	0.0	–	–
	0.483	0.429 ± 0.05	89.0
	0.965	1.06 ± 0.10	109
	2.41	2.39 ± 0.14	99.0
Mineral water (Damavand)	0.0	–	–
	0.483	0.349 ± 0.08	73.0
	0.965	1.04 ± 0.10	107
	2.41	2.37 ± 0.10	98.2
Potable tap water	0.0	–	–
	0.483	0.511 ± 0.05	106
	0.965	0.864 ± 0.16	89.5
	2.41	2.29 ± 0.16	95.2
Tea	0.0	–	–
	0.483	0.449 ± 0.11	93.0
	0.965	0.787 ± 0.05	81.5
	2.41	2.32 ± 0.23	96.2
Rice	0.0	–	–
	0.483	0.415 ± 0.04	86
	0.965	1.00 ± 0.24	104
	2.41	2.27 ± 0.29	94.0

Results are presented as the mean ± standard deviation ($n=5$)

4 Conclusion

Among different analytical methods, fluorescent sensors have been praised as notably effective protocols for determining trace metal ions with the advantages of convenience, instantaneous response, selectivity, and high sensitivity. Carbon dots, one of the most efficient and stable nanoprobes, are recently used as chemical sensors for different types of analytes owing to their easy preparation, good water solubility, photostability, low toxicity, and biocompatibility. In the current study, the N–S co-doped CDs were directly prepared within 2.5 min and in one step by microwave heating as an easy and economical method. Also, tri-ammonium citrate and thiourea were used as cheap and available precursors. The FT-IR analysis confirmed the presence of oxygen-containing functional groups in CDs. The EDX analysis also showed the elemental composition of 59.57, 13.99, 24.30, and 2.13%wt of C, N, O, and S, respectively. From the initial evaluations, it is evident that Pb(II) could quench the fluorescence of CDs with higher quenching efficiency compared to other studied ions. Further, the CDs were characterized analytically as a sensor for Pb(II) detection in the aqueous solution. The results showed high selectivity toward Pb(II) ions, and the sensor was successfully used for Pb(II) analysis in food samples.

Supplementary Information The online version contains supplementary material available at https://doi.org/10.1007/s42823-023-00529-9.

Acknowledgements The authors appreciate the support of the Ferdowsi University of Mashhad (No. 3/54203).

Author contributions All authors contributed to the study conception and design. The first draft of the manuscript was prepared by Elias Aboobakri and all authors commented on previous versions of the manuscript. All authors read and approved the final manuscript. EA: investigation, data curation, writing—original draft. TH: supervision, methodology, formal analysis, investigation, review and editing of the original draft. MJ: supervision, methodology, resources, review and editing of the original draft.

Funding The authors do not receive a specific project grant but this work was supported by the block grant available to the Ferdowsi University of Mashhad received by Elias Aboobakri as a Ph. D candidate.

Data availability All data generated or analyzed during this study are included in this manuscript.

Code availability A statement regarding code availability is not applicable.

Declarations

Conflict of interest The authors declare that they have no conflict of interest.

Ethical approval This article does not contain any studies with human or animal subjects.

Consent to participate Not applicable.

Consent for publication The authors hereby consent to the publication of the work.

References

1. Qu J, Yuan Y, Zhang X, Wang L, Tao Y, Jiang Z, Yu H, Dong M, Zhang Y (2022) Stabilization of lead and cadmium in soil by sulfur-iron functionalized biochar: Performance, mechanisms and microbial community evolution. J Hazard Mater 425:127876. https://doi.org/10.1016/j.jhazmat.2021.127876
2. Payehghadr M, Esmaeilpour S, Kazem Rofouei M, Adlnasab L (2013) Determination of trace amount of cadmium by atomic absorption spectrometry in table salt after solid phase preconcentration using octadecyl silica membrane disk modified by a new derivative of pyridine. J Chem 2013:1–6. https://doi.org/10.1155/2013/417085
3. Qu J, Wei S, Liu Y, Zhang X, Jiang Z, Tao Y, Zhang G, Zhang B, Wang L, Zhang Y (2022) Effective lead passivation in soil by bone char/CMC-stabilized FeS composite loading with phosphate-solubilizing bacteria. J Hazard Mater 423:127043. https://doi.org/10.1016/j.jhazmat.2021.127043
4. Wang Z-X, Yu X-H, Li F, Kong F-Y, Lv W-X, Fan D-H, Wang W (2017) Preparation of boron-doped carbon dots for fluorometric determination of Pb(II), Cu(II) and pyrophosphate ions. Microchim Acta 184:4775–4783. https://doi.org/10.1007/s00604-017-2526-3
5. Salmanipour A, Taher MA (2011) An electrochemical sensor for stripping analysis of Pb(II) based on multiwalled carbon nanotube functionalized with 5-Br-PADAP. J Solid State Electrochem 15:2695–2702. https://doi.org/10.1007/s10008-010-1197-3
6. Deka MJ, Chowdhury D, Nath BK (2022) Recent development of modified fluorescent carbon quantum dots-based fluorescence sensors for food quality assessment. Carbon Lett 32:1131–1149. https://doi.org/10.1007/s42823-022-00347-5
7. Ju H, Lee MH, Kim J, Kim JS, Kim J (2011) Rhodamine-based chemosensing monolayers on glass as a facile fluorescent "turn-on" sensing film for selective detection of Pb2+. Talanta 83:1359–1363. https://doi.org/10.1016/j.talanta.2010.11.016
8. Srisukjaroen R, Wechakorn K, Teepoo S (2022) A smartphone based-paper test strip chemosensor coupled with gold nanoparticles for the Pb2+ detection in highly contaminated meat samples. Microchem J 179:107438. https://doi.org/10.1016/j.microc.2022.107438
9. Li G, Belwal T, Luo Z, Li Y, Li L, Xu Y, Lin X (2021) Direct detection of Pb2+ and Cd2+ in juice and beverage samples using PDMS modified nanochannels electrochemical sensors. Food Chem 356:129632. https://doi.org/10.1016/j.foodchem.2021.129632
10. Sharma P, Mehata MS (2020) Rapid sensing of lead metal ions in an aqueous medium by MoS2 quantum dots fluorescence turn-off. Mater Res Bull 131:110978. https://doi.org/10.1016/j.materresbull.2020.110978
11. Baker SN, Baker GA (2010) Luminescent carbon nanodots: emergent nanolights. Angew Chem Int Ed 49:6726–6744. https://doi.org/10.1002/anie.200906623
12. Liu R, Zhang Y, Piao Y, Meng L-Y (2021) Development of nitrogen-doped carbon quantum dots as fluorescent probes for highly selective and sensitive detection of the heavy-ion Fe3+. Carbon Lett 31:821–829. https://doi.org/10.1007/s42823-020-00222-1
13. Wee SS, Ng YH, Ng SM (2013) Synthesis of fluorescent carbon dots via simple acid hydrolysis of bovine serum albumin and its potential as sensitive sensing probe for lead (II) ions. Talanta 116:71–76. https://doi.org/10.1016/j.talanta.2013.04.081
14. Silva J, Gonçalves H (2011) Analytical and bioanalytical applications of carbon dots. TrAC, Trends Anal Chem 30:1327–1336. https://doi.org/10.1016/j.trac.2011.04.009
15. Qu J, Bi F, Hu Q, Wu P, Ding B, Tao Y, Ma S, Qian C, Zhang Y (2023) A novel PEI-grafted N-doping magnetic hydrochar for enhanced scavenging of BPA and Cr(VI) from aqueous phase. Environ Pollut 321:121142. https://doi.org/10.1016/j.envpol.2023.121142
16. Hou J, Li H, Wang L, Zhang P, Zhou T, Ding H, Ding L (2016) Rapid microwave-assisted synthesis of molecularly imprinted polymers on carbon quantum dots for fluorescent sensing of tetracycline in milk. Talanta 146:34–40. https://doi.org/10.1016/j.talanta.2015.08.024
17. Pan D, Zhang J, Li Z, Wu C, Yan X, Wu M (2010) Observation of pH-, solvent-, spin-, and excitation-dependent blue photoluminescence from carbon nanoparticles. Chem Commun 46:3681–3683. https://doi.org/10.1039/C000114G
18. Gupta A, Verma NC, Khan S, Tiwari S, Chaudhary A, Nandi CK (2016) Paper strip based and live cell ultrasensitive lead sensor using carbon dots synthesized from biological media. Sens Actuators B 232:107–114. https://doi.org/10.1016/j.snb.2016.03.110
19. Aboobakri E, Jahani M (2020) Graphene oxide/Fe3O4/polyaniline nanocomposite as an efficient adsorbent for the extraction and preconcentration of ultra-trace levels of cadmium in rice and tea samples. Res Chem Intermed 46:5181–5198. https://doi.org/10.1007/s11164-020-04256-y
20. Wang B, Zhuo S, Chen L, Zhang Y (2014) Fluorescent graphene quantum dot nanoprobes for the sensitive and selective detection of mercury ions. Spectrochim Acta Part A 131:384–387. https://doi.org/10.1016/j.saa.2014.04.129
21. Pajewska-Szmyt M, Buszewski B, Gadzała-Kopciuch R (2020) Sulphur and nitrogen doped carbon dots synthesis by microwave assisted method as quantitative analytical nano-tool for mercury ion sensing. Mater Chem Phys 242:122484. https://doi.org/10.1016/j.matchemphys.2019.122484
22. He JH, Cheng YY, Yang T, Zou HY, Huang CZ (2018) Functional preserving carbon dots-based fluorescent probe for mercury (II) ions sensing in herbal medicines via coordination and electron transfer. Anal Chim Acta 1035:203–210. https://doi.org/10.1016/j.aca.2018.06.053
23. Zhang Y, Cui P, Zhang F, Feng X, Wang Y, Yang Y, Liu X (2016) Fluorescent probes for "off–on" highly sensitive detection of Hg2+ and L-cysteine based on nitrogen-doped carbon dots. Talanta 152:288–300. https://doi.org/10.1016/j.talanta.2016.02.018
24. Wei J-M, Liu B-T, Zhang X, Song C-C (2018) One-pot synthesis of N, S co-doped photoluminescent carbon quantum dots for Hg2+ ion detection. New Carbon Mater 33:333–340. https://doi.org/10.1016/S1872-5805(18)60343-9
25. Yu P, Wen X, Toh Y-R, Tang J (2012) Temperature-dependent fluorescence in carbon dots. J Phys Chem C 116:25552–25557. https://doi.org/10.1021/jp307308z
26. Liu Y, Liu CY, Zhang ZY (2011) Synthesis and surface photochemistry of graphitized carbon quantum dots. J Colloid Interface Sci 356:416–421. https://doi.org/10.1016/j.jcis.2011.01.065
27. Bao L, Liu C, Zhang Z-L, Pang D-W (2015) Photoluminescence-tunable carbon nanodots: surface-state energy-gap tuning. Adv Mater 27:1663–1667. https://doi.org/10.1002/adma.201405070
28. Jalili R, Amjadi M (2015) Surface molecular imprinting on silane-functionalized carbon dots for selective recognition of nifedipine. RSC Adv 5:74084–74090. https://doi.org/10.1039/C5RA12189B
29. Chen Y, Wu Y, Weng B, Wang B, Li C (2016) Facile synthesis of nitrogen and sulfur co-doped carbon dots and application for Fe(III) ions detection and cell imaging. Sens Actuat B. 223:689–696. https://doi.org/10.1016/j.snb.2015.09.081

30. Sun M, Qu J, Han T, Xue J, Li K, Jiang Z, Zhang G, Yu H, Zhang Y (2023) Resource utilization of bovine bone to prepare biochar as persulfate activator for phenol degradation. J Cleaner Prod 383:135415. https://doi.org/10.1016/j.jclepro.2022.135415
31. Barati A, Shamsipur M, Arkan E, Hosseinzadeh L, Abdollahi H (2015) Synthesis of biocompatible and highly photoluminescent nitrogen doped carbon dots from lime: analytical applications and optimization using response surface methodology. Mater Sci Eng C 47:325–332. https://doi.org/10.1016/j.msec.2014.11.035
32. Hou Y, Lu Q, Deng J, Li H, Zhang Y (2015) One-pot electrochemical synthesis of functionalized fluorescent carbon dots and their selective sensing for mercury ion. Anal Chim Acta 866:69–74. https://doi.org/10.1016/j.aca.2015.01.039
33. Wang W, Damm C, Walter J, Nacken T, Peukert W (2015) Photobleaching and stabilization of carbon nanodots produced by solvothermal synthesis. Phys Chem Chem Phys. https://doi.org/10.1039/C5CP04942C
34. Xiong W, Zhou L, Liu S (2016) Development of gold-doped carbon foams as a sensitive electrochemical sensor for simultaneous determination of Pb (II) and Cu (II). Chem Eng J 284:650–656. https://doi.org/10.1016/j.cej.2015.09.013
35. Fu X, Lou T, Chen Z, Lin M, Feng W, Chen L (2012) "Turn-on" fluorescence detection of lead ions based on accelerated leaching of gold nanoparticles on the surface of graphene. ACS Appl Mater Interfaces 4:1080–1086. https://doi.org/10.1021/am201711j
36. Molaei MJ (2020) Principles, mechanisms, and application of carbon quantum dots in sensors: a review. Anal Methods 12:1266–1287. https://doi.org/10.1039/C9AY02696G
37. Li W, Hu X, Li Q, Shi Y, Zhai X, Xu Y, Li Z, Huang X, Wang X, Shi J, Zou X, Kang S (2020) Copper nanoclusters @ nitrogen-doped carbon quantum dots-based ratiometric fluorescence probe for lead (II) ions detection in porphyra. Food Chem 320:126623. https://doi.org/10.1016/j.foodchem.2020.126623
38. Liu Y, Zhou Q, Yuan Y, Wu Y (2017) Hydrothermal synthesis of fluorescent carbon dots from sodium citrate and polyacrylamide and their highly selective detection of lead and pyrophosphate. Carbon 115:550–560. https://doi.org/10.1016/j.carbon.2017.01.035
39. Wang Q, Zhang S, Ge H, Tian G, Cao N, Li Y (2015) A fluorescent turn-off/on method based on carbon dots as fluorescent probes for the sensitive determination of Pb2+ and pyrophosphate in an aqueous solution. Sens Actuat B 207:25–33. https://doi.org/10.1016/j.snb.2014.10.096
40. Jiang Y, Wang Y, Meng F, Wang B, Cheng Y, Zhu C (2015) N-doped carbon dots synthesized by rapid microwave irradiation as highly fluorescent probes for Pb2+ detection. New J Chem 39:3357–3360. https://doi.org/10.1039/C5NJ00170F
41. Liu Y, Zhou Q, Li J, Lei M, Yan X (2016) Selective and sensitive chemosensor for lead ions using fluorescent carbon dots prepared from chocolate by one-step hydrothermal method. Sens Actuat B 237:597–604. https://doi.org/10.1016/j.snb.2016.06.092
42. Tabaraki R, Sadeghinejad N (2018) Microwave assisted synthesis of doped carbon dots and their application as green and simple turn off–on fluorescent sensor for mercury (II) and iodide in environmental samples. Ecotoxicol Environ Saf 153:101–106. https://doi.org/10.1016/j.ecoenv.2018.01.059